Dissipative mechanisms in the 120 MeV $^{19}F+^{64}Ni$ reaction

F. Terrasi, A. Brondi, G. La Rana, G. De Angelis, A. D'Onofrio, R. Moro,
E. Perillo, and M. Romano
Dipartimento di Scienze Fisiche dell'Università and Istituto Nazionale di Fisica Nucleare, I-80125 Napoli, Italy
(Received 6 March 1989)

Energy spectra and angular distributions of projectile-like fragments, ranging from ^{7}Be to ^{18}O, have been measured for the 120 MeV $^{19}F+^{64}Ni$ reaction. Experimental evidence is given for the presence of two dissipative components attributed, on the basis of optimum Q values, to incomplete fusion and deep-inelastic collision mechanisms. Measured Q-value spectra show the dominance of the incomplete fusion mechanism in N and O isotopes production, while deep-inelastic collisions increase with the charge transfer. Furthermore, angular distributions and optimum Q values display larger relative contributions of incomplete fusion with respect to deep inelastic collisions for heavier isotopes of each Z. An incomplete fusion model reproduces the cross sections for most of the channels where this mechanism is prevalent. An attempt to include deep inelastic mechanisms in the same model is presented.

I. INTRODUCTION

Dissipative mechanisms in heavy-ion-induced reactions have been largely studied in the past years over a wide range of energies and with different projectile-target combinations. They can be essentially grouped in two main categories: deep-inelastic collisions (DIC) and incomplete fusion (IF) or massive transfer.

Deep-inelastic collisions, observed mainly in reactions between heavy nuclei, are characterized by the dissipation of most of the total kinetic energy of the colliding nuclei into intrinsic excitations. The formation of an intermediate rotating system has been demonstrated by several studies.[1,2] In particular, the sticking model has been successfully applied in many cases. In reactions between medium-light nuclei at relatively low-energy the DIC cross section is significantly smaller and shows many features resembling those observed in reactions induced by heavy projectiles on heavy targets at higher energy. In the case of a 120 MeV $^{30}Si+^{30}Si$ reaction[3] the measured Q values and cross sections strongly indicated the presence of DIC in the production of fragments close to the projectile.

Incomplete fusion reactions indicate a class of dissipative mechanisms, observed essentially in rather asymmetric systems with heavy targets, which exhibit characteristics of direct reactions. The energy dissipation involved in this process is significantly smaller compared to the case of DIC (Ref. 4), indicating a much faster time scale. Incomplete fusion mechanisms have recently been studied in reactions between medium-light nuclei.[5–8] An incomplete fusion model proposed by Wilczynski[9] provided, in many cases, guidance to understanding the process. In this picture the IF channels are localized in narrow windows in the peripheral region of l space. At the same time, cross sections are governed by phase space, where only the radial part of the available energy is dissipated.[10]

Many questions are still open about these two processes, especially for light systems at low bombarding energy. They concern the coexistence and the competition between them, and the transition from one mechanism to the other. Both mechanisms have been observed in the system 120 MeV $^{30}Si+^{30}Si$ (Ref. 3). A transition was found from IF, responsible for large massive transfers, to DIC, which dominates for small mass transfers. The interplay between quasielastic and deep-inelastic reactions has also been studied (Ref. 11) for the systems $^{46,48,50}Ti+^{208}Pb$ at $E_{c.m.}=243$ MeV. In this case the situation is reversed: Quasielastic channels are prevalent for the heaviest fragments emission, while deep-inelastic collisions dominate for large massive transfers. Furthermore, two different mechanisms have been observed at forward and backward angles, respectively, for the reaction 140 MeV $^{19}F+^{89}Y$ (Ref. 12).

In this framework we have undertaken the study of dissipative mechanisms in the 120 MeV $^{19}F+^{64}Ni$ reaction, by measuring the projectile-like fragments spectra and angular distributions. The aim was to gain insight on the incomplete fusion, which is expected to dominate in this reaction, and deep-inelastic collisions. We have used the incomplete fusion model proposed by Wilczynski[9,10] to interpret the measured Q values and the angle-integrated cross sections. Finally, a simple approach to account for the DIC mechanism in this model is presented and discussed.

II. EXPERIMENTAL PROCEDURE AND RESULTS

A self-supporting target of ^{64}Ni enriched to 96%, 500 $\mu g/cm^2$ thick, was bombarded by a 120 MeV ^{19}F beam, provided by the XTU Tandem of the Laboratori Nazionali di Legnaro. Average beam current was ≈ 50 enA. Integrated charge was measured by an electron-suppressed Faraday cup.

Ejectile energy spectra were measured using two three stage Si telescopes covering the angular ranges 15°–35° and 35°–55°, respectively, in steps of 5°. The classical

 ©1989 The American Physical Society

grazing angle for this reaction is $\theta^{lab}_{graz} \simeq 21°$. The detector thicknesses were 50, 500, and 5000 μm for the first telescope and 21, 95, and 3000 μm for the second one. Energy thresholds for C isotopes were $\approx$42 MeV for the first telescope and $\approx$24 MeV for the second one. The solid angle subtended by the detectors was 1.7 msr. In the entire angular range a good nuclear charge separation was obtained up to $Z=9$ ejectiles. Due to its larger first-stage thickness, the first telescope allowed both Z and A identification for all the observed ejectiles in the entire energy range. The energy calibration was accomplished for each Si detector by a pulse generator normalized to the peak due to the 5.48 MeV alpha-particle decay of ^{241}Am and by the elastic scattering of ^{19}F beam from the target. A good agreement between the two calibrations was obtained.

Off-line analysis of two-dimensional spectra, performed using a microVax, yielded the energy spectra at different

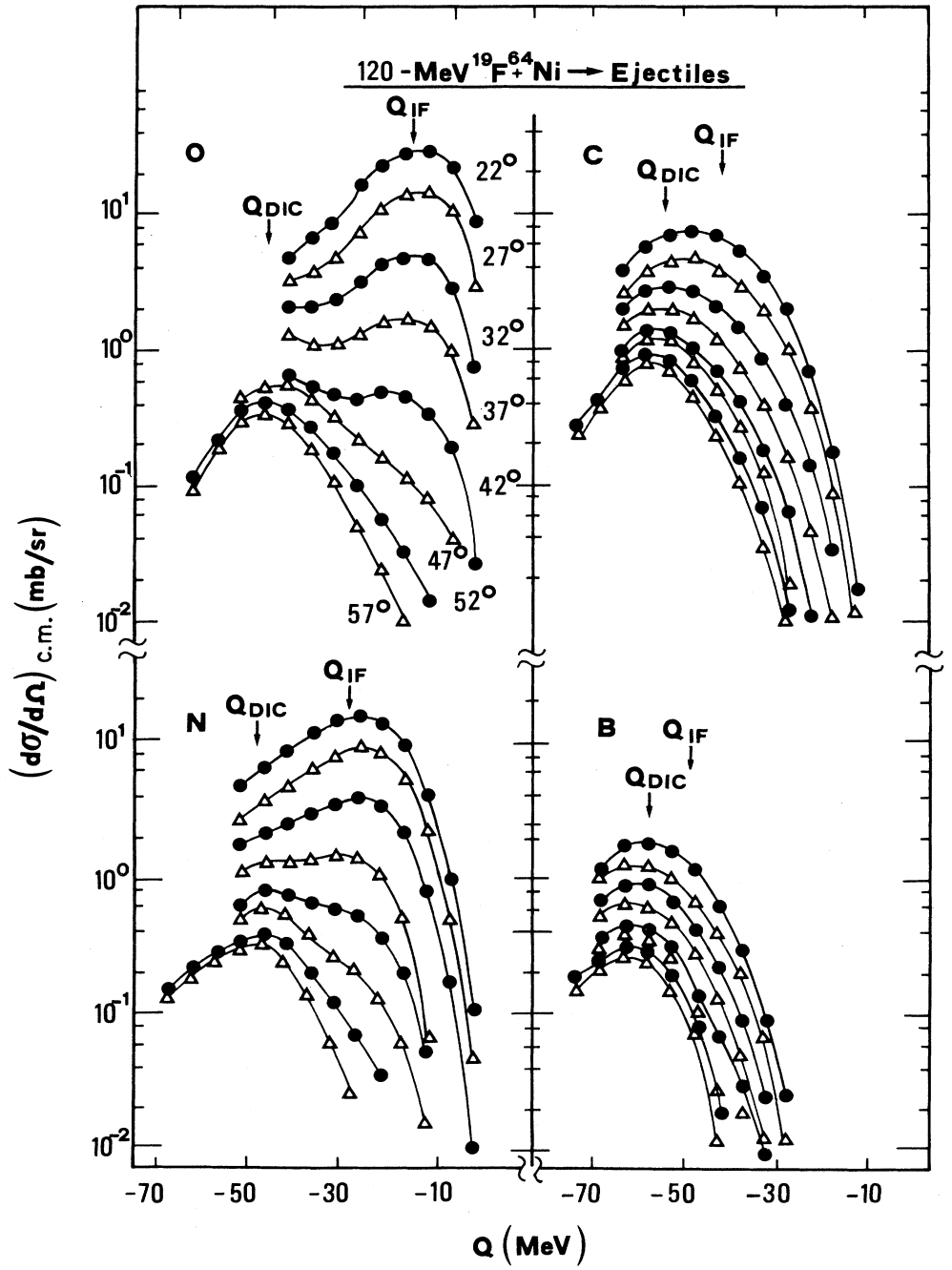

FIG. 1. Absolute Q spectra measured at different angles in the center-of-mass system for the ejectiles B, C, N, and O emitted in the reaction 120 MeV $^{19}F+^{64}Ni$. The arrows indicate the results of a calculation of optimum Q value for deep-inelastic collisions (Q_{DIC}) and for incomplete fusion mechanism (Q_{IF}).

TABLE I. Comparison between measured optimum Q values (Q_{IF}^{exp},Q_{DIC}^{exp}) for the observed ejectiles with those calculated for incomplete fusion mechanism (Q_{IF}) and for deep-inelastic collisions in the sticking limit (Q_{DIC}). Average values of orbital angular momenta ($\langle l \rangle$) deduced from an incomplete fusion model are also reported.

Ejec.	$\langle l \rangle$ ($\hbar$)	$\lvert Q_{IF} \rvert$ (MeV)	$\lvert Q_{IF}^{exp} \rvert$ (MeV)	$\lvert Q_{DIC} \rvert$ (MeV)	$\lvert Q_{DIC}^{exp} \rvert$ (MeV)
B	50.2	52.0	60.0[a]	59.0	
C	52.3	43.0	47.0[a]	54.0	
N	55.8	31.0	28.0	50.0	47.0
O	60.9	16.0	13.0	47.0	47.0

[a]See text.

angles for each identified ejectile. Angle-integrated cross sections were obtained integrating numerically the angular distributions, extrapolated to the full angular range.

A. Z-identified ejectiles

Measured absolute Q spectra for ejectiles with $Z=5,6,7,8$ at eight angles in the center-of-mass system are shown in Fig. 1. The laboratory center-of-mass transformation was accomplished by a double linear interpolation procedure in the E-θ plane. Optimum Q values, which correspond to the maxima in the energy spectra, have been extracted. They show that, if an energy sharing between the two fragments proportional to their masses is assumed, the possible light-particle evaporation from the primary light fragments can be neglected for all the observed ejectiles. For the most forward angles ($\theta_{c.m.}=22°$, 27°, 32°, and 37°) the experimental thresholds did not allow us to explore the region for $|Q| \gtrsim 50$ MeV for O and N spectra, and $|Q| \gtrsim 70$ MeV for B and C ejectiles.

The presence of two components corresponding to different optimum Q values can be observed in O and N spectra. The less dissipative component dominates at forward angles, while the other one dominates at larger angles. These two components will be referred to as IF and DIC in the following. In fact, as it will be shown in Sec. III, they can be identified as due to incomplete fusion and deep-inelastic processes. For B and C ejectiles they appear not to be separated, and no dominance of one with respect to the other is observed. A similar behavior has previously been observed for 100 MeV $^{16}O+^{64}Ni$ reaction.[6] Between the two different components, the IF one dominates in the production of O and N ejectiles. Optimum Q values extracted from Q spectra are reported in the fourth and sixth columns of Table I. For O and N ejectiles the maxima of the two components are reported, while for B and C the maximum of the spectrum ($|Q_{IF}^{exp}|$) has to be considered as an optimum Q value intermediate between those expected for the two components.

Measured angle-integrated cross sections, summed over the different isotopes for each Z, are shown in Fig. 2 (circles with error bars), for all the observed ejectiles. A total cross section for the production of ejectiles between Be and O has been obtained: $\sigma_{Be\text{-}O}=(730\pm200)$ mb. The large error bars include uncertainties in the extrapolation of the measured angular distributions to the entire angular range, as well as those related to experimental energy thresholds.

B. Z- and A-identified ejectiles

As previously mentioned, the telescope used at forward angles allowed isotope mass separation, and therefore center-of-mass angular distributions of Z- and A-identified ejectiles in the angular range 22°–42° could be obtained (Fig. 3). For N and O ejectiles they are strongly peaked at forward angles confirming the dominance of the IF mechanism found in the analysis of Q-value spectra for the Z channels. On the other hand, Be, B, and C angular distributions are indicative of more dissipative processes, as we observe anisotropies significantly smaller. This is consistent with the indications obtained by Q-

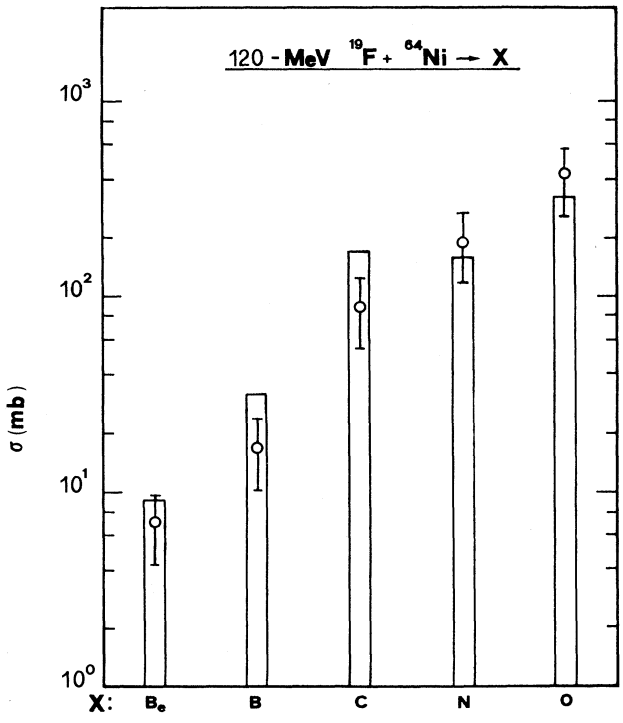

FIG. 2. Measured angle-integrated cross sections for the observed ejectiles compared with the predictions of the incomplete fusion model (Ref. 9) (full lines).

value spectra that DIC contributions become more important in these channels.

Except for O ejectiles, there is evidence, for each Z, that the anisotropies are correlated with the isotope mass: We observe that channels corresponding to small mass transfers present higher contributions of direct mechanisms (i.e., IF). This behavior is more evident in Fig. 4 where we show the angular distributions measured for $^{12,13,14}C$ and $^{14,15,16}N$ ejectiles, gated by different Q-value windows. The total angular distributions are also shown for comparison. The Q-value windows have been chosen to select regions where the relative contribution of the two identified mechanisms appears significantly different (see Fig. 1). As it can be seen, the relative weight is strongly related to the isotope mass for both ejectiles. In particular, increasing the mass transfer (i.e., for lighter ejectiles), the contribution of DIC with respect to IF increases; this effect becomes particularly strong for N ejectiles. Looking at the angular dependence, we observe that the ratio of the cross section in the more dissipative Q-value window to that in the less dissipative window becomes larger at backward angles, as expected.

The same behavior concerning the sharing of the cross section between DIC and IF processes for different mass isotopes can be recognized in the optimum Q values. The experimental Q values, reported in the fourth column of Table II, show a strong decrease with increasing mass transfer, for given Z, which can be related to the increasing weight of the more dissipative mechanism. Absolute angle-integrated cross sections for all Z- and A-identified

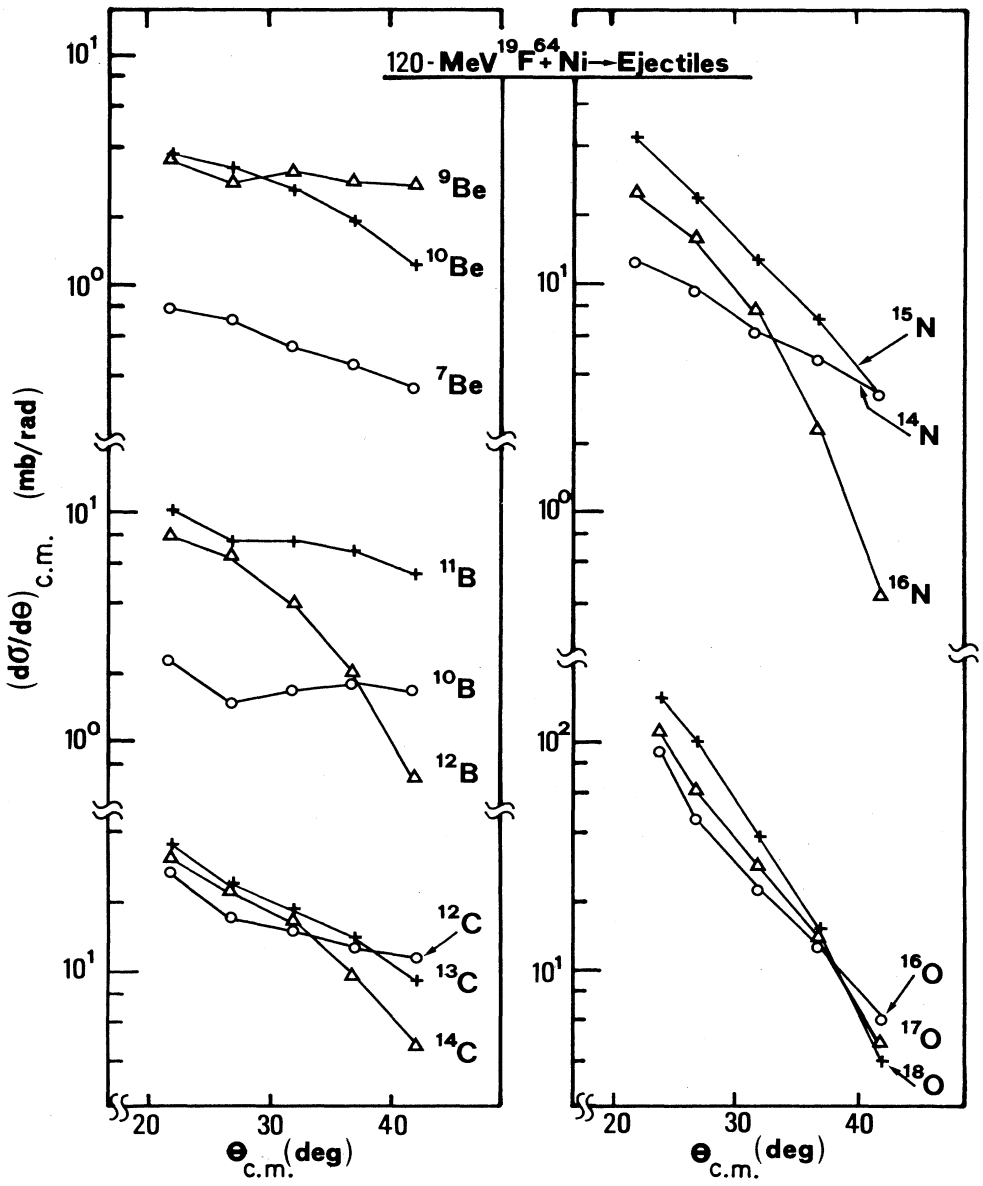

FIG. 3. Center-of-mass angular distributions measured for Z- and A-identified ejectiles (full lines are drawn to guide the eye).

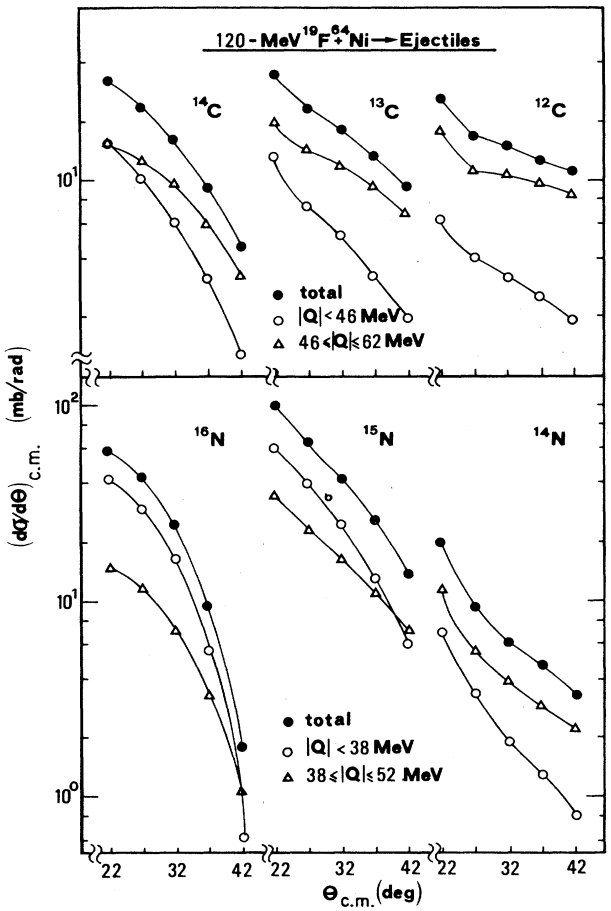

FIG. 4. Center-of-mass angular distributions measured for $^{12,13,14}C$ and $^{14,15,16}N$ ejectiles, gated by different Q-value windows.

ejectiles have been extracted and are shown in Fig. 5 as circles with error bars.

III. ANALYSIS OF DATA IN TERMS OF TWO REACTION MECHANISMS

From the data presented in the preceding section, a quasielastic mechanism appears to be prevalent in the ejectile emission cross section in the system under study, although a more dissipative process is also present. Therefore, we have compared our data with the predictions of an IF model, which uses the prescription proposed by Wilckzynski,[10] as far as the optimum Q values are concerned, and the sum-rule model presented in Ref. 9 for the emission cross sections.

In Sec. III A we discuss the comparison of model predictions with mass-integrated data in the whole investigated angular range. The behavior of experimental data for Z- and A-identified ejectiles at forward angles is presented in Sec. III B. From the available information, the need to take into account for IF and DIC processes in the same context is derived. A simple approach to accomplish this task is presented in Sec. III C.

TABLE II. Comparison between measured optimum Q values (Q^{exp}) for Z- and A-identified ejectiles with those calculated for incomplete fusion mechanism (Q_{IF}) and for deep-inelastic collisions in the sticking limit (Q_{DIC}). Average values of orbital angular momenta ($\langle l \rangle$) deduced from an incomplete fusion model are also reported.

Ejec.	$\langle l \rangle$ ($\hbar$)	$\lvert Q_{IF} \rvert$ (MeV)	$\lvert Q^{exp} \rvert$ (MeV)	$\lvert Q_{DIC} \rvert$ (MeV)
$^{7}_{4}Be$	48.0	63.0	68.0	63.0
$^{9}_{4}Be$	48.6	60.0	63.0	64.0
$^{10}_{4}Be$	48.9	58.0	62.0	64.0
$^{10}_{5}B$	50.0	53.0	60.0	58.0
$^{11}_{5}B$	50.4	51.0	56.0	58.0
$^{12}_{5}B$	50.6	49.0	52.0	59.0
$^{12}_{6}C$	52.0	44.0	50.0	53.0
$^{13}_{6}C$	52.6	42.0	46.0	54.0
$^{14}_{6}C$	53.0	39.0	42.0	55.0
$^{14}_{7}N$	55.2	34.0	42.0	50.0
$^{15}_{7}N$	56.0	30.0	30.0	50.0
$^{16}_{7}N$	56.5	27.0	27.0	51.0
$^{16}_{8}O$	59.7	20.0	20.0	46.0
$^{17}_{8}O$	61.4	14.0	16.0	47.0
$^{18}_{8}O$	62.8	9.0	10.0	48.0

A. Z dependence of optimum Q values and cross sections

The arrows in Fig. 1 indicated by Q_{IF} and Q_{DIC} represent the results of two calculations: The first one is an l-dependent optimum Q value calculated according to Ref. 10, while the second calculation provided an optimum Q value for deep-inelastic collisions in the sticking limit.

For Q_{DIC} calculations the l window from $l_{crit}=42\hbar$ to $l_{graz}=68\hbar$ has been used. The value of l_{crit} for fusion has been calculated using the Krappe, Nix, and Sierk potential,[13] while the value of $l_{graz}=68\hbar$ has been calculated using the Wilcke parametrization[14] and is in agreement with the quarter point angle resulting from the analysis of the angular distribution of elastic scattering.

The rotational energy of the dinuclear complex is calculated assuming an angular momentum $J=f\langle l \rangle$ where f is the sticking factor[15] and $\langle l \rangle$ is the average angular momentum in the assumed l window. The moment of inertia of the rotating system is calculated using the half-density radii where

$$R_i=1.28A_i^{1/3}-0.76+0.8A_i^{-1/3}$$

(Ref. 16). The barrier seen by the two fragments at the scission point is calculated using the nuclear potential proposed by Wilczynski.[17]

Optimum Q values for IF have been calculated using the l-dependent expression proposed in Ref. 10. In this picture the nucleon transfers occur in peripheral collisions in narrow windows of partial waves. Therefore, the optimum Q value is related to an optimum l value in the entrance channel, with the assumption that the radial part of the kinetic energy at the interaction distance is converted into intrinsic excitations and that the tangential energy is scaled according to the recoil formula of Siemens.[18] The barrier heights in the entrance and exit

channels have been calculated by means of the same potential used in DIC calculations, with the interaction radius from Ref. 17. The optimum l values have been calculated in the frame of the sum-rule model proposed in Ref. 9.

The basis of the sum-rule model resides in two physical ingredients: (a) The partial statistical equilibrium reached by the dinuclear complex during the nucleon transfer, which provides the Q_{gg}-ΔQ_C (Ref. 19) dependence of the cross section, where ΔQ_C is the difference in Coulomb energy between exit and entrance channels of the reaction and Q_{gg} is the ground-ground Q value; (b) The generalized concept of critical angular momentum which allows the transfer of a cluster from the projectile to the target (or from the target to the projectile) only if the relative orbital angular momentum of the subsystem (cluster plus target or projectile) is smaller than the corresponding critical angular momentum for fusion. This condition determines a localization of the IF in l space.

Sum-rule calculations have been performed including all the reaction channels for which the corresponding Q_{gg} values are available in the recent mass table of Wapstra and Audi.[20] l_{crit}'s for the fusion of each transferred cluster with the target (or projectile) have been calculated using the prescription given in Ref. 9. The three parameters,[9] effective temperature T, diffuseness in l space a, and the interaction radius parameter R_0 used in the calculation are $T=3.0$ MeV, $a=0.5\hbar$, and $R_0=1.5$ fm, respectively. These parameters have been taken to reproduce the total measured cross section $\sigma^{th}_{Be\text{-}O}=745$ mb ($\sigma^{exp}_{Be\text{-}O}=730$ mb). It must be pointed out that this latter constraint is rather severe and it is relevant as far as the sharing of the cross section over the observed channels is concerned.

In Fig. 6 we present the calculated cross section for complete and incomplete fusion channels versus the orbital angular momentum in the entrance channel, for most of the observed ejectiles. In the upper part of the figure the complete fusion and the most intense IF channels are shown. As it can be seen, there is a relatively strong dependence of the l localization on Z. On the bottom of the same figure the A dependence of the cross-section distribution is shown. Although the integrated cross sections are strongly dependent on A for a given Z, the average l is only little affected by A, except for O ejectiles which are emitted in l windows around the l_{graz}.

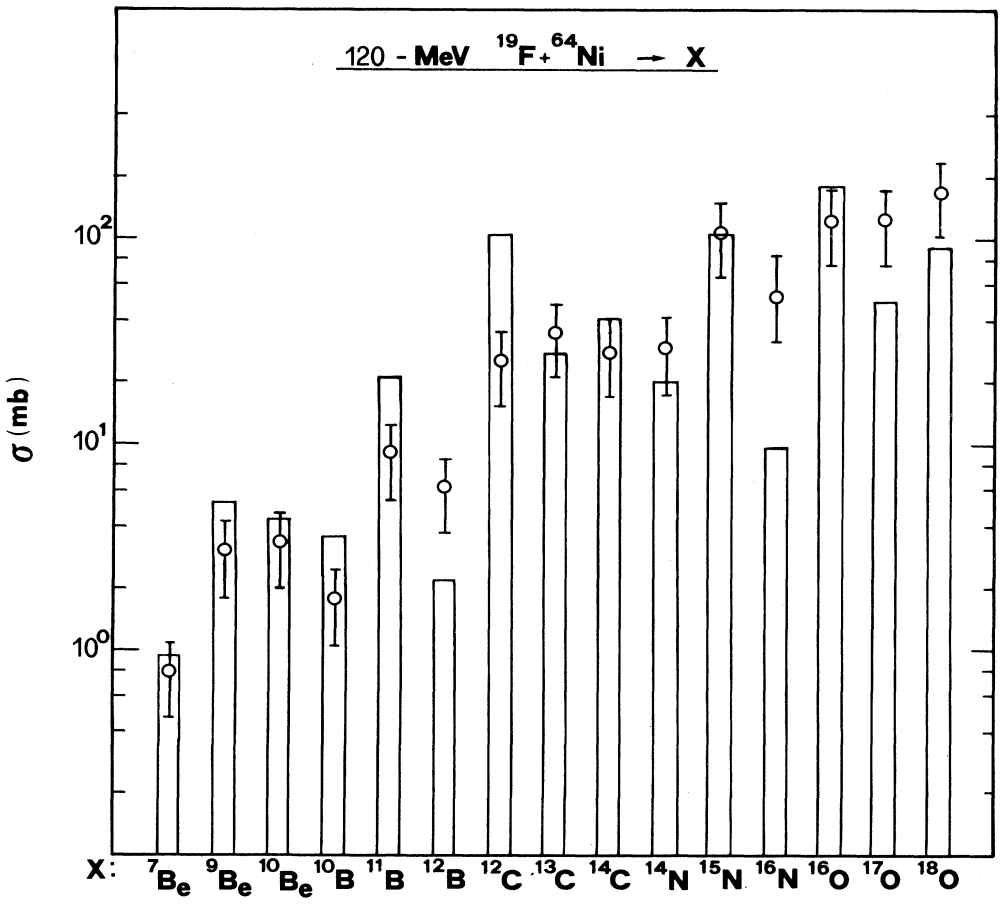

FIG. 5. Measured angle-integrated cross sections for Z- and A-identified ejectiles compared with the prediction of the incomplete fusion model (Ref. 9) (full lines).

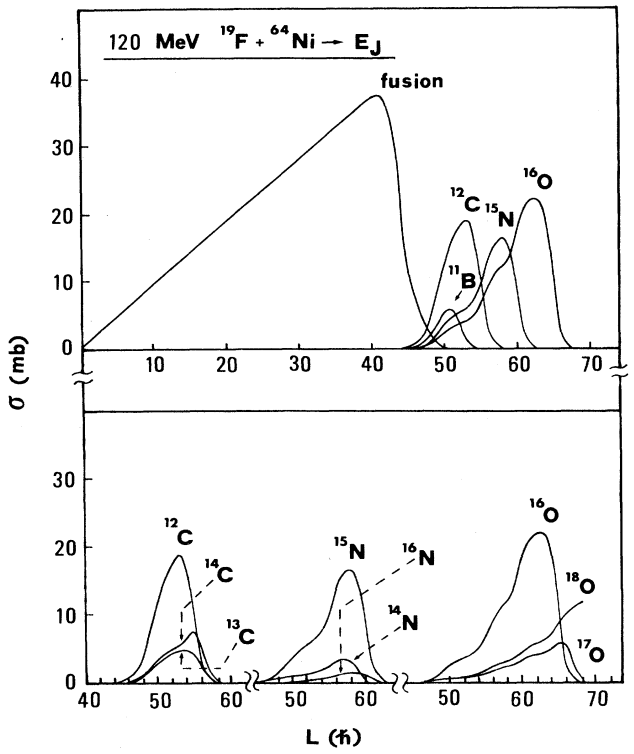

FIG. 6. Calculated angle-integrated cross sections versus the orbital angular momentum in the entrance channel for the complete fusion and most of the observed incomplete fusion channels.

The average l's of the cross-section distributions, summed over the different isotopes for a given Z, are presented in Table I and they have been used for determining optimum Q values for IF.

The comparison between the predicted optimum Q values for DIC and IF mechanisms and the data in Fig. 1 strongly indicates the presence of these two mechanisms in the ejectile production. This indication appears very clear in the case of N and O, where two peaks are observed in the Q spectra (Fig. 1) and their maxima are well accounted for by the calculation. For B and C these two components do not appear to be separated. A qualitative trend of the relative weight of these two components can be deduced from Fig. 1: The IF contribution with respect to the DIC one decreases when the mass transfer increases. For B ejectiles, DIC contribution appears larger than the IF one, reversing the situation encountered for N and O ejectiles. Similar conclusions can be deduced from Table I where a comparison between experimental and calculated Q values is shown.

As far as the experimental cross sections are concerned, Fig. 2 shows an exponential increase as a function of Z. This behavior is partially accounted for by the IF model whose predictions are shown in Fig. 2 as full lines. In fact, the model reproduces well the cross sections for N and O, while a significant discrepancy is observed for B and C ejectiles.

B. A dependence of optimum Q values and cross sections

In Table II we compare experimental optimum Q values (Q^{exp}) measured for Z- and A-identified ejectiles with those calculated for incomplete fusion (Q_{IF}) and deep-inelastic collisions (Q_{DIC}). The optimum l values calculated by the sum-rule model are also reported. The good agreement observed between Q^{exp} and Q_{IF} for N and O isotopes indicates that the model reproduces the dependence of energy dissipation on isotope mass. For ^{14}N a discrepancy is observed, which can be ascribed to the DIC mechanism which begins to be significant. For C isotopes the experimental Q values lie between the two calculated ones, suggesting a comparable contribution of the two mechanisms. Q values become closer to Q_{DIC} when the mass transfer increases, indicating the corresponding increase of this mechanism.

Most of the measured angle-integrated cross sections, shown in Fig. 5, are essentially concentrated on $^{15,16}N$ and $^{16,17,18}O$ emission. As already discussed in Sec. III A, the cross section decreases, on the average, when the mass transfer increases. The full lines represent the predictions of the sum-rule model,[9] using the parameters mentioned in the preceding paragraph. Owing to the fact that the DIC mechanism is not included in this model, we expect to reproduce the cross sections better for the channels where IF dominates, i.e., for N and O isotopes. As a matter of fact, most of N and O cross sections are reproduced by the model except for ^{16}N, for which a significant discrepancy is found. For more massive

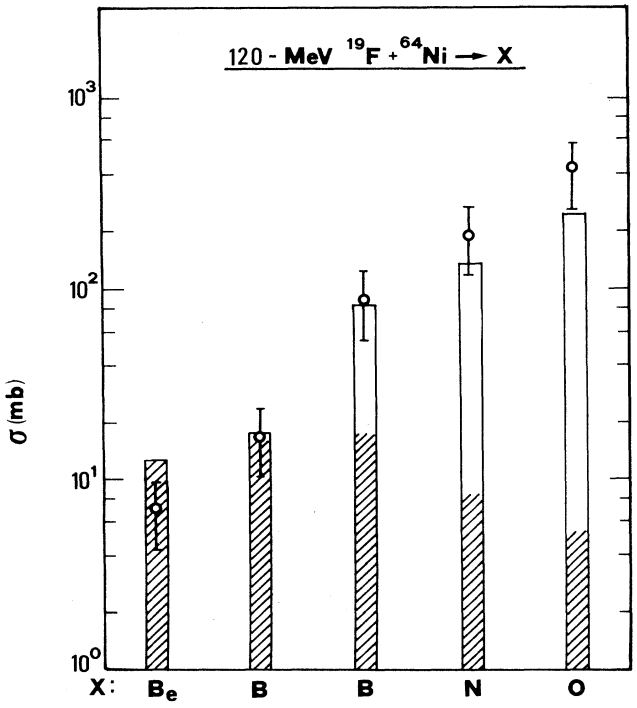

FIG. 7. Measured angle-integrated cross sections for the observed ejectiles compared with the predictions of a modified sum-rule model including both IF and DIC mechanisms (full lines). DIC contributions are indicated by hatched areas.

transfers where the DIC component becomes stronger, large deviations are present for ^{12}C, ^{12}B, ^{11}B, and ^{9}Be. The overestimation of the model for the ^{12}C cross section appears particularly large.

In order to understand which are the driving physical ingredients of the model, several calculations have been performed to unfold the effects due to the localization in l space and to the phase-space term appearing in the probability factor[9]

$$P(i)=\exp\{[Q_{gg}(i)-\Delta Q_C(i)]/T\} , \quad (1)$$

where $Q_{gg}(i)-\Delta Q_C(i)$ represents the excitation energy of the heavy partner in the hypothesis of no kinetic-energy dissipation at the interaction distance. The l localization alone implies upper limits for l distributions of IF channels increasing from l_{crit} to l_{graz}, when going from complete fusion to neutron transfer, providing a slight increase of the cross section with the ejectile mass. The exponential trend of the cross section with the mass transfer is therefore due to the combined effects of l localization and of the phase-space term (1) which determines the competition between the IF channels. The different Q_{gg}'s of different isotopes, for each Z, modulate the cross-section values.

An accurate comparison of the A dependence of the measured isotope cross sections for each Z reveals a significant deviation from the expected Q_{gg} dependence. The foregoing discrepancies cannot be eliminated adjusting the sum-rule parameters. On the other hand, the inclusion in the expression (1) of the radial kinetic-energy dissipation better describes the physical situation of a direct mechanism, where a partial statistical equilibrium is reached;[14]

$$P(i,l)=\exp\{[Q_{gg}(i)-Q_{IF}^{rad}(i,l)]/T\} ,$$
$$Q_{IF}^{rad}(i,l)=\Delta Q_C(i)-(E_0-U_0)(1-l_i^2/l_{graz}^2) , \quad (2)$$

where E_0 is the center-of-mass incident energy, U_0 is the barrier height in the entrance channel, and l_i is the angular momentum for channel i. The effects of this correction turn out to be rather small.

C. A simple approach to include DIC in the sum-rule model

The analysis in terms of Q values indicates the presence of another mechanism, besides IF, which we have identified as DIC. At the same time, the previously discussed discrepancies between measured and calculated cross sections could be ascribed to the coexistence of both mechanisms. A similar comparison for the system 120 MeV $^{30}Si+^{30}Si$ allowed us to interpret the data in terms

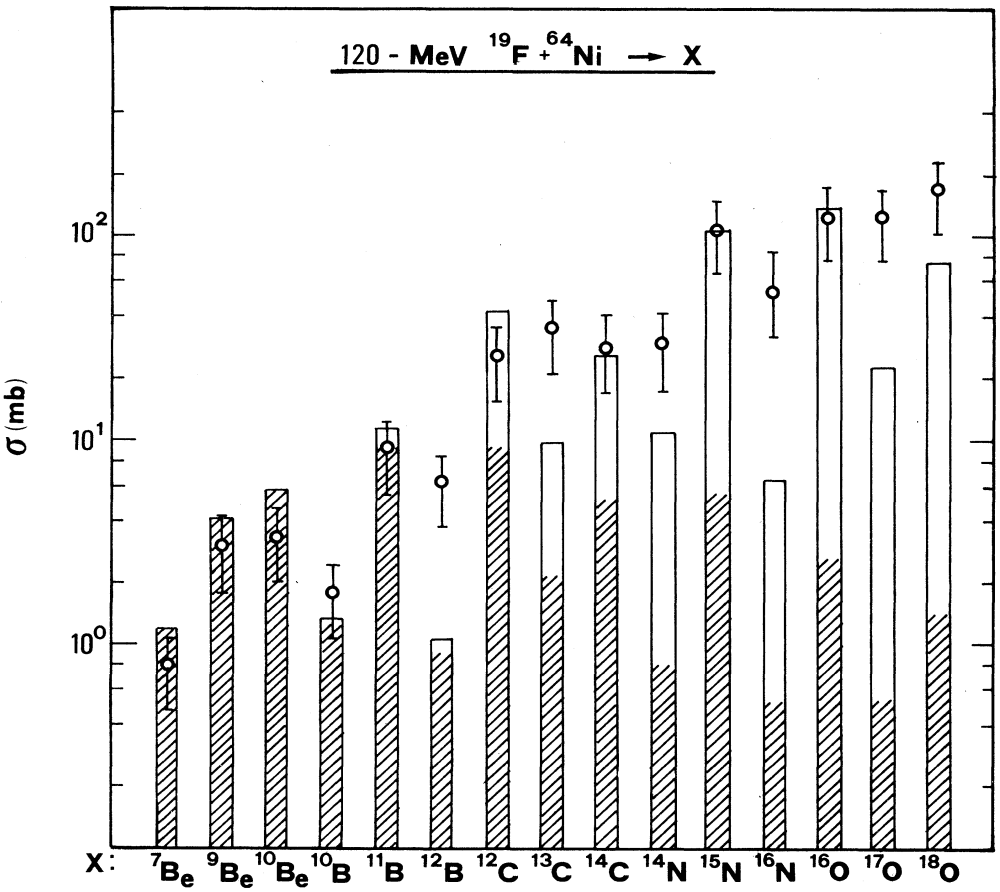

FIG. 8. Same as Fig. 7 but for Z- and A-identified ejectiles.

of the coexistence of both DIC and IF. In that case[3] DIC, representing most of the cross section, were concentrated at small mass transfers, while IF appeared to be responsible for large massive transfers. In the present system the situation is reversed: IF mechanisms dominate and produce essentially ejectiles close to the projectile. This behavior may be related to the higher degree of mass asymmetry in the entrance channel compared to the system studied in Ref. 3. In our case the deviations found between data and the sum-rule model are smaller than those found in Ref. 3, but the indications obtained from the analysis of Q values and angular distributions have suggested to include DIC in the sum-rule model. Building a model which accounts for all the aspects of both mechanisms is out of the aim of this paper. Nevertheless, the very simple approach we are presenting here to account for DIC in the sum-rule model may provide further insights on these two mechanisms.

In our approach DIC processes are treated on the same footing as IF. In particular, the competition between DIC channels has been derived by a phase-space term, similar to expression (2), in which the Q values calculated for each l in the sticking limit appear instead of $Q_{\rm IF}^{\rm rad}(i,l)$. On the other hand, allowing DIC to compete with the IF in all the $l_{\rm crit}$-$l_{\rm graz}$ window, the former would dominate for all the ejectiles, as $Q_{\rm DIC}$'s are significantly larger than $Q_{\rm IF}$'s. The foregoing considerations have suggested to confine DIC mechanisms in a low l region in the $l_{\rm crit}$-$l_{\rm graz}$ window. In this region the term (2) makes the DIC process dominant with respect to IF, which occurs in a more peripheral l window.

The regions $l_{\rm crit}$-$l_{\rm DIC}=42-52\hbar$ and $l_{\rm crit}$-$l_{\rm graz}=42-68\hbar$ were used, respectively, for DIC and IF in the calculation which follows. With this choice of $l_{\rm DIC}$, Be, and B ejectiles will be produced essentially by the DIC mechanism (see Fig. 6), as for $l>52\hbar$, IF contributes very little to such channels. Moreover, for C ejectiles (see bottom of Fig. 6) more than half of the cross section will result from IF, the remaining part competing with DIC channels. For N and O ejectiles DIC contribution becomes small, leaving room for IF which becomes the dominant mechanism.

The result of the calculation is shown in Figs. 7 and 8 as a full line for Z and A,Z channels, respectively. DIC contributions to the cross section are indicated by hatched regions in the rectangles. The IF parameters used in the calculation described in the preceding subsections have been retained. For DIC a higher temperature $T_{\rm DIC}=3.5$ has been used. Comparing these results with those obtained assuming only incomplete fusion (Fig. 5) we observe a substantial improvement for ^{9}Be and ^{10,11}B. For ^{12}C there is a significant reduction in the deviation between data and the calculation, but still we do not obtain a good agreement. For N and O ejectiles, as expected, the situation remains rather unchanged, except that a small reduction of the cross section is produced, due to the strong competition with DIC channels for $l<52\hbar$. For ^{13}C the calculation is not able to predict the cross section, and at the same time the discrepancy between data and calculation for ^{12}B is increased compared to the calculation including only IF. According to this model the resulting total cross section for DIC, as far as the observed channels are concerned, is $\sigma_{\rm DIC}=59$ mb.

The optimum l values for IF and relative Q values derived from these calculations show essentially no variation for O and N ejectiles with respect to the values obtained assuming only IF, while a reduction of 1–2 MeV is obtained for the other ejectiles. Although we do not obtain a remarkable improvement in the agreement between data and calculations for all channels, compared to the calculation including only IF, we can conclude that this simple model describes qualitatively well the observed coexistence of the two mechanisms in this system and the transition from one mechanism to the other as a function of the mass transfer.

IV. SUMMARY AND CONCLUSIONS

Ejectile emission in the reaction ^{19}F+^{64}Ni at 120 MeV bombarding energy has been studied. Energy spectra and angular distributions for Z-identified projectile-like fragments between Be and O have been measured in the angular range 15°–55° in the laboratory system. For the most forward angles (15°–35°) A identification was possible for all fragments.

Incomplete fusion and deep-inelastic collisions have been found to compete with increasing relative weight going from Be to O ions. An interesting correlation between the sharing of the cross section between these two mechanisms and the mass transfer has been observed in the angular distributions.

The comparison between measured optimum Q values and cross sections for each ejectile with the prediction of an incomplete fusion model shows a reasonable agreement, which has been partially improved introducing the competition between IF and DIC in the model. In particular, experimental data indicate that DIC are mainly concentrated in an angular momentum window between $l=42\hbar$ ($l_{\rm crit}$ for complete fusion) and $52\hbar$, thus giving rise to the predominance of such a reaction mechanism for the lighter ejectiles. On the other hand, IF processes are responsible for N and O channels, which occur essentially for $l>52\hbar$. For this reason a good agreement of the data with the original IF model for these ejectiles was already obtained.

In conclusion, we would like to emphasize that the need to treat incomplete fusion and deep-inelastic collisions in the same context had already emerged from several studies, besides the present one. A realistic model for the description of both mechanisms is a formidable task, as dynamical aspects, besides the phase space, are very important in the description of such processes. Nevertheless, the simple approach presented here can be considered a quantitative scheme useful to extract the overall behavior of the competition between IF and DIC as a function of the entrance-channel mass asymmetry, incident energy, etc. On the other hand, these results encourage further refinements of the model.

We wish to thank all the members of the staff of the XTU Tandem at the Laboratori Nazionali di Legnaro and Alfonso Boiano for his technical support to the experiment.

[1]C. Ngô, in *Phenomenological Approaches of Dissipative Heavy Ion Collisions,* edited by Le Service de documentation, Centre d'Etudes nucleàires de Saclay (91191 Gif-sur-Yvette, France, 1983), p. 33.

[2]W. U. Schroder and J. R. Huizenga, in *Treatise on Heavy Ion Science,* edited by D. A. Broomley (Plenum, New York, 1985), Vol. 2, and references therein.

[3]R. Moro, G. La Rana, A. Brondi, P. Cuzzocrea, A. D'Onofrio, E. Perillo, M. Romano, F. Terrasi, E. Vardaci, and H. Dumont, Nucl. Phys. **A477**, 120 (1988).

[4]R. H. Siemssen, Nucl. Phys. **A400**, 245c (1983).

[5]H. Ikezoe, N. Shikazono, Y. Tomita, K. Ideno, Y. Sugiyama, and E. Takekoshi, Nucl. Phys. **A444**, 349 (1985).

[6]A. Brondi, G. Cavaccini, A. D'Onofrio, G. La Rana, R. Moro, V. Roca, M. Romano, G. Spadaccini, F. Terrasi, and M. Vigilante, Nucl. Phys. **A489**, 547 (1988).

[7]D. J. Parker, J. Asher, T. W. Conlon, and I. Naqib, Phys. Rev. C **30**, 143 (1984).

[8]H. Morgenstern, W. Bohne, K. Grabisch, D. G. Kovar, and H. Lehr, Phys. Lett. **113B**, 463 (1982).

[9]J. Wilczynski, K. Siwek-Wilczynska, J. Van Driel, S. Gonggrijp, D. C. J. M. Hageman, R. V. F. Janssens, J. Lukasiak, R. H. Siemssen, and S. Y. van der Werf, Nucl. Phys. **A373**, 109 (1982).

[10]J. Wilczynski, in *Proceedings of the International Conference on Nuclear Physics, Florence, 1983,* edited by R. A. Ricci and P. Blasi (Tipografia Compositori, Bologna, 1983), p. 305.

[11]K. E. Rehm, A. M. van den Berg, J. J. Kolata, D. G. Kovar, W. Kutschera, G. Rosner, G. S. F. Stephans, and J. L. Yntema, Phys. Rev. C **37**, 2629 (1988).

[12]T. Suomijarvi, R. Lucas, M. C. Mermaz, J. P. Coffin, G. Guillaume, B. Heusch, F. Jundt, and F. Rami, Z. Phys. A **321**, 531 (1985).

[13]H. J. Krappe, J. R. Nix, and A. J. Sierk, Phys. Rev. C **20**, 992 (1979).

[14]W. W. Wilcke, J. R. Birkelund, H. J. Wollersheim, A. D. Hoover, J. R. Huizenga, W. U. Schroder, and L. Tubbs, At. Data Nucl. Data Tables **25**, 389 (1980).

[15]R. Bass, in *Nuclear Reactions with Heavy Ions,* edited by W. Beiglbock, E. H. Lieb, M. Goldhaber, and W. Thirring (Springer, Berlin, 1980), p. 89.

[16]W. U. Schroder and J. R. Huizenga, Annu. Rev. Nucl. Sci. **27**, 465 (1977).

[17]J. Wilczynski and K. Siwek-Wilczynska, Phys. Lett. **55B**, 270 (1975).

[18]P. J. Siemens, J. P. Bondorf, D. H. E. Gross, and F. Dickmann, Phys. Lett. **36B**, 24 (1971).

[19]J. P. Bondorf, F. Dickmann, D. H. E. Gross, and P. J. Siemens, J. Phys. (Paris), Colloq. **32**, Suppl. 11-12, C6-145 (1971).

[20]A. H. Wapstra and G. Audi, Nucl. Phys. **A432**, 1 (1985).